Thematic mapping and atmospheric correction of aerospace images

V.V. Belov, S.V. Afonin, Yu.V. Gridnev, and K.T. Protasov

Institute of Atmospheric Optics,
Siberian Branch of the Russian Academy of Sciences, Tomsk

Received July 9, 1999

Some results of researches carried out in the Institute of Atmospheric Optics on the problems of thematic analysis and atmospheric correction of spaceborne images of the Earth surface, obtained for the visible and IR spectral ranges, are briefly reviewed.

Introduction

The Geological Information System (GIS) technologies, as powerful and convenient means of storing, processing, and interpreting environmental information, frequently use, as a basis, archived (or multiyear observational) data on the environmental conditions. Changes in the environmental components are identified by comparison of the information from this base with the data of operative observations over these components. For the global-scale components (e.g., atmosphere, ocean, forests, continental coastal line, glaciers as a global water reservoir, etc.), the aerospace systems still remain the only means of operative control of their properties on the global or regional scale. In recent years the role of observations from satellites has rapidly increased. The reasons for this are as follows.

In the last few decades, considerable progress has been achieved in the development of efficient opto-electronic ground-based systems[1] with high resolution (spatial, spectral, etc.). Owing to their high level of automation and ability of acquiring information in real time, these remote-sensing systems may in some cases provide as accurate estimates of the environmental processes as their "*in situ*" counterparts.

Another one reason for a rapid growth of the number of satellite product users, though not federally organized, is an easy access to the operative satellite information. In Russia and other CIS members, this happened because of the efforts of the Russian Space Agency, Institute of Space Research RAS, and ScanEx firm which organized production and distribution of relatively cheap portable systems, that can be controlled with commercially available computers, for preliminary processing of data from NOAA meteorological satellites (USA) and satellites of Resource series (Russia).

Despite the satellites have already for decades been used by many national and international environmental research projects, the whole problem of reliable interpretation of satellite data is still far from being solved. For instance, the data of satellite monitoring of the atmosphere obtained using opto-electronic remote sensing techniques are frequently illustrative or qualitative and not more. In their turn, the quantitative estimates whose accuracy is unclear are often of a limited practical use.

Good quantitative results can be obtained with satellite methods of remote sensing of sea surface temperature. However, the results obtained in the coastal zones typically are not processed because of the absence of algorithms taking the land effect into account.

Distorting effect of the atmosphere on the satellite images of the Earth's surface

Any satellite image of the Earth is in fact a superposition of signals coming from (1) surface region being viewed; (2) atmosphere overlying the region; and (3) atmosphere–surface system as a result of interaction of optical radiation with the atmosphere and reflection from the surface. For instance, in infrared region, satellites receive radiation emitted by the Earth's surface and atmosphere and, in addition, surface-emitted upwelling radiation and surface-reflected radiation. In other words, the satellite/aircraft imagery data on the Earth simultaneously contain information on the optical properties of the Earth's surface and the atmosphere. Therefore, the opto-electronic systems developed for study, retrieval, and monitoring of surface properties must be used under conditions when the atmospheric effect is minimized, and vice versa when the atmosphere itself is to be studied.

In many practical applications, the instrumentation frequently fails to eliminate completely the adverse atmospheric effect on accuracy of analysis or thematic mapping of the information extracted from satellite data. In these cases, modules supplementary to automatic image processing facilities are employed for atmospheric correction. The atmospheric correction is difficult to make, primarily because the atmospheric conditions at the time of experiment are usually unknown. Fortunately, advances in space-based lidar sensing of the atmosphere offer new possibilities of correctly interpreting the results obtained with passive opto-electronic measurement systems from space. Specifically,

0235-6880/99/10 951-06 $02.00

they may provide necessary information on the optical state of the atmosphere at the time of the measurement and, thus, to make more correct interpretation of the satellite observations of the Earth's surface.

We will present two most obvious examples of how the effect of atmospheric distortions on the accuracy of retrievals of surface properties from satellite data can be mitigated using data (e.g., from airborne lidar) on the optical state of the atmospheric channel at the measurement time.

The first example (Fig. 1) is reproduced from Ref. 2 and shows how aerosol atmosphere influences the performance of image-recognition routine in thematic mapping of multichannel Landsat data. Shown in the figure, from left to right, are the following episodes:

1) a sampling scene (containing a pond surrounded by not mowed bean field);

2) the spectral traits of the water and bean field in the fourth to seventh channels of the opto-electronic sensor on Landsat satellite; and

3) the spectral traits of the image including

– sampled scene (dotted-dashed curve);

– pond against sand background (solid curve); and

– mowed wheat field against the sand background.

Evidently, the water against bean background will be misinterpreted due to the atmospheric effect, as the mowed wheat field. It is important that this result has been obtained under conditions of a moderately turbid cloudless atmosphere. This example is a direct evidence of the capabilities of aerospace monitoring of the surface biosphere state, including forest service issues among others.

The second example is based on the results of the study on detecting small-scale thermal surface anomalies using infrared satellite imagery data. Figure 2 shows that the scattering properties of the atmosphere may strongly distort the satellite-derived characteristics (e.g., sizes) of small-scale surface temperature anomalies. Removing this interference can facilitate early detection of the anomalies, so that timely measures can be undertaken against such hazardous events as forest fires.

Satellite monitoring of atmospheric aerosol using data of AVHRR radiometer

The space-based techniques have proven to be an efficient tool of operational remote monitoring of atmospheric aerosol. Recently, new algorithms have been developed for retrieval of aerosol optical depth τ_a from data of AVHRR radiometers installed on NOAA satellites at visible wavelengths; using them, a lot of data on global τ_a distribution over the world ocean regions have been accumulated.[5,6] However, the utility of these algorithms for aerosol monitoring over land and inland water basins and for identifying aerosol types is still unclear. It goes without saying that, the infrared imagery, when used together with its visible counterparts, improves the performance of aerosol monitoring technique during daytime and forms a good basis for detection of local aerosol features at night.

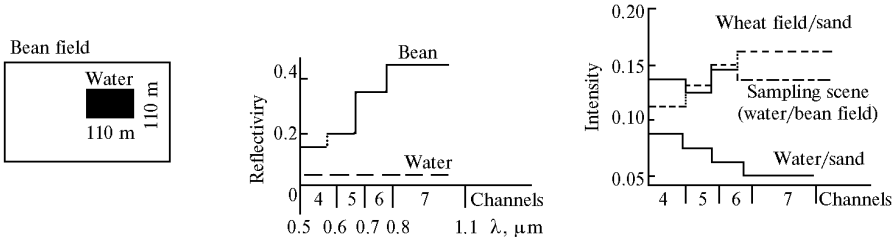

Fig. 1. Modification of the spectral image and recognition of a sampling scene on the Earth surface as viewed from space (in 4 optical channels of Landsat satellite) through the aerosol atmosphere of moderate turbidity.

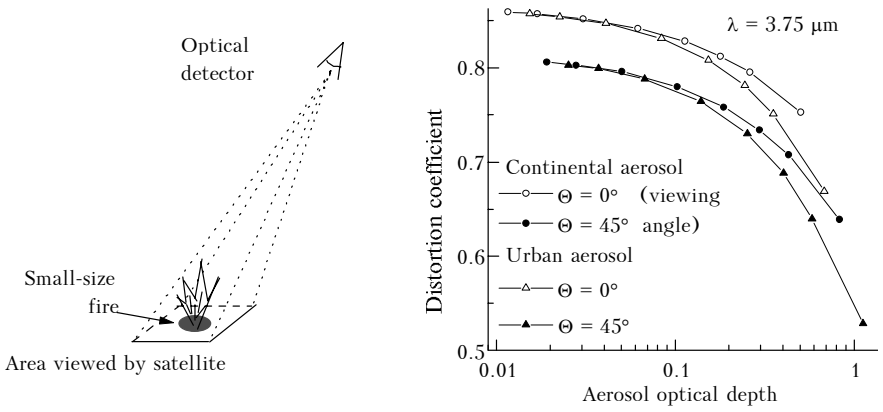

Fig. 2. Coefficient of atmospheric distortion of the fire linear size.

The possibility of using the infrared imagery for detection of surface areas where near-ground atmospheric layer has enhanced aerosol turbidity, and for identification of aerosol type, has been explored at the Institute of Atmospheric Optics. This was done numerically by imitating, for midlatitude summer conditions, the nighttime and daytime radiance (brightness temperature) measurements of upward going thermal radiation in the infrared 3 (3.55–3.93 μm), 4 (10.3–11.3 μm), and 5 (11.5–12.5 μm) channels of an AVHRR radiometer. The computations were made assuming nonreflecting underlying surface and different aerosol types (rural, urban) in the near-ground layer, and by using (a) "standard" midlatitude summer vertical profiles of meteorological parameters and surface temperatures (T_s = 294 K) and (b) "nonstandard" low surface temperatures (T_s = 278 K, such as those over the Lake " aikal).

Under "standard" conditions, the infrared AVHRR channels have rather low sensitivity to variations of the optical characteristics of the near-ground aerosol. For instance, at infrared wavelengths in the third channel the brightness temperature variations do not exceed 0.8–1.7 K with the increasing τ_a, 1.0–2.0 K in the fourth channel, and 0.7–1.2 K in the fifth channel. Setting the threshold for the brightness temperature difference ("clean" minus "turbid") at 0.5 K, only regions with strong atmospheric turbidities corresponding to meteorological visibility range S_m < 3–5 km can be detected. On the other hand, when the surface temperature is low compared to "standard" case, the infrared channels are much more sensitive to τ_a variations in the near-ground layer (because of a stronger influence of aerosol on the upward going flux of thermal radiation in this case), with the corresponding maximum variations of brightness temperatures due to τ_a fluctuations being 4.5–6.0 K in the third channel, 2.2–3.0 K in the fourth channel, and 1.5–2.3 K in the fifth channel.

Hence, in this case the regions with turbidity S_m ~ 10–15 km can readily be detected. At the same time, because the nighttime observational data on continental and urban aerosols differ only a little, the infrared satellite imagery can hardly be used to identify the aerosol type.

In the 3.55–3.93 μm channel, the aerosol scattering of solar radiation is stronger at daytime than nighttime hours; consequently, the brightness temperature is higher, but the emission from the atmosphere–surface system is weaker (since aerosol optical depth is larger) at daylight hours.

Hence, the measurements in the channel will depend on τ_a variations, and this dependence will be sensitive to two competing effects as well as to solar zenith angle, aerosol type, and surface temperature. The highest sensitivity will be observed in the presence of continental aerosol at low surface temperatures: as τ_a varies, the maximum change in brightness temperature may be (a) 0.9–3.3 K for continental aerosol and only 0.1–0.8 K when conditions are "standard" and the sun angle between 15 and 60°; and (b) it is 6.7–10.6 K for continental aerosol and only 6.6–8.8 K for urban aerosol under conditions with low T_s.

Thus, in some extreme cases, the daytime measurements in the 3.55–3.93 μm channel may be less sensitive to τ_a variations than do nighttime observations. Overall, the use of this IR channel for detection of local regions with increased turbidity may be more efficient during daytime than at night. At sun angles about 60° and low T_s levels, the detection limit may be S_m = 20–25 km as high, but under standard conditions it may drop to S_m = 5–8 km for continental aerosol, and even to 1–2 km for an urban aerosol.

When measurements in the 3.55–3.93 μm channel are used to identify aerosol type, the dependence on solar elevation angle and azimuth of viewing direction should be taken into account adequately. Ideally, the brightness temperature ranges for different aerosol types should not overlap. The numerical simulations showed that for the continental and urban aerosols this is the case when solar zenith angle is between 15 and 60°. Of course, the aerosol type can be successfully identified only when optical and geometrical observation conditions allow one to do this. The atmospheric turbidity should be strong enough, i.e., S_m has to be no larger than 10 km.

These theoretical results have been confirmed experimentally by analysis of actual IR images of the Lake " aikal and collocated ground-based data.[7]

Evaluation of satellite-based methods of forest fire detection from AVHRR data

The increasing use of space-based instruments by operational systems of forest fire detection raises the need in more efficient algorithms of automatic identification of high-temperature anomalies.

Current fire detection systems widely use the five-channel AVHRR radiometers installed onboard NOAA meteorological satellites, which can be used for operative monitoring of potentially fire dangerous conditions over vast territories throughout the world several times a day. Fire detection algorithms frequently employ threshold techniques as described in Refs. 8–10, which compare radiances of the upward going radiation or their combinations with some preset thresholds. In particular, the atmospheric distortion of optical radiation is corrected for by specially selected thresholds. The main informative features, used in these fire detection algorithms, are the brightness temperatures in the third channel ($T3$) and the temperature difference ($T3 - T4$) between third and fourth channels. Other combinations of radiances recorded from a satellite are used to identify atmospheric (cloud) cover in order to reduce the number of false alarms.

The accuracy of threshold methods is determined by the optical and geometrical conditions during the

observations as well as by the sun-satellite viewing geometry. To see how these factors influence performance of fire detection algorithms, we have intercompared four threshold techniques[8–10] using model and measured (in summer of 1998) data for a forested area in Tomsk region. Model results were generated by using the LOWTRAN–7 code that we have modified a little bit, whereas experimental data for the summer of 1998 were extracted from archive.

Let $A1$ and $A2$ denote the albedo in channels 1 and 2; $R1 = A1/\cos(\mathrm{SZA})$, $R2 = A2/\cos(\mathrm{SZA})$, where SZA is the solar zenith angle; $T3$, $T4$, and $T5$ are brightness temperatures in the channels 3, 4, and 5, respectively; $dT34 = T3 - T4$; $dT45 = T4 - T5$; $dT3S = T3 - [T4 + 3.303(T4 - T5)]$. Using this designations, we will describe the tests used in some threshold techniques.[8–10]

Algorithm 1 (Ref. 9) (used by CCM ICZF S" RAS):

(a) identifies fires during night

$A1 < 1$, $T3 > 290$ K, $T4 > 265$ K, $dT3S > 4$ K;

(b) identifies large fires during daytime under any observation conditions

$A1 < 25$, $T3 > 320$ K, $T4 > 265$K, $dT3S > 4$ K;

(c) identifies fires during daytime in the presence of thin clouds

$A1 < 10$, $T3 > 316$ K, $dT3S > 4$ K;

(d) identifies fires during daytime under clear-sky conditions

$A1 < 4$, $T3 > 306$ K, $dT3S > 4$ K.

Algorithm 2 (Ref. 10) (designed by ScanEx firm)

$R1 < 20$, A" $S(R1 - R2) > 2$, $T3 > 318$ K, $dT34 > 10$ K, $T4 > 270$ K.

Algorithm 3 (Ref. 8) (after Kaufman et al., 1990–1994):

$A1 < 20$, $T3 > 315$ K, $dT34 > 8$ K, $T4 > 265$ K.

Algorithm 4 (Ref. 8) (after Franca et al., 1993)

$A1 < 9$, $T3 > 320$ K, $dT34 > 15$ K, $0 < dT45 < 5$, $T4 > 287$ K.

The algorithms were validated against officially available data, provided by the Aviation base of forest fire protection, on detection times and other characteristics of forest fires. Some results of this comparison are presented in Tables 1 and 2. Runs of the algorithm under model fire conditions have shown that:

1) when fires have large size, the individual threshold techniques differ insignificantly (with the exception of the one proposed in Ref. 10) in terms of their predictions;

2) in most cases, the CCM ICZF S" RAS algorithm performs best of all[9]; and

3) at the edges of the radiometer scans, the efficiency of an algorithm depends essentially on the fire size: it changes insignificantly for large fires, but for the task of early detection of small fires even efficiency of the best algorithm among those considered above may degrade by an order of magnitude relative to nadir viewing case.

These conclusions are supported by results on testing the algorithms against the field (archived) data, with most important findings being as follows:

1) the algorithm from Ref. 9 performs best of all;

2) although quite efficient for fire detection, the algorithm of Ref. 8 (after Kaufman) produced relatively large false alarm errors, particularly during July observations;

3) operator-corrected results for August 1998 gave the highest probability of early forest fire detection from AVHRR data; so this proved very efficient method (operator plus algorithm[9]) of the forest fire monitoring;

4) for algorithms considered here, the minimum detectable burning area is about 0.2–0.4 ha.

Table 1. Model cases. Intercomparison among the threshold algorithms

Algorithm	Viewing angle, in deg.				
	0	30	40	45	50
	Burning area 10000 m^2				
1	391/303	321/255	311/245	294/228	247/181
2	153/120	110/88	93/77	75/65	46/37
3	398/310	314/248	308/242	301/235	242/176
4	303/237	292/233	247/192	197/150	97/60
	Burning area 400 m^2				
1	242/176	107/78	35/21	22/13	12/3
2	93/63	–	–	–	–
3	198/132	11/5	–	–	–
4	160/97	–	–	–	–
Area, m^2	Algorithm (Ref. 9)				
200	121/88	33/23	18/9	4/3	1/1
100	40/28	13/3	3/3	1/1	–
50	16/4	2/2	–	–	–

Note. Presented are the total numbers of optical-geometrical situations when algorithm detected fire/including those detected through the cloudy layers.

Table 2. Results of field tests of the satellite algorithms of forest fire detection

Algorithm	Number of pixels identified, %		Fires detected		Fires detected earlier	
	July	August	July	August	July	August
Operator	79.2	83.9	46(5)	67(8)	8(1)	38(3)
1	89.8	89.6	32(3)	47(3)	8(3)	19(1)
2	90.2	88.6	21(2)	31(2)	3(1)	8(0)
3	63.8	85.0	45(9)	46(3)	9(3)	12(0)
4	90.6	88.3	18(1)	29(2)	3(1)	8(0)

Note. Given in parentheses are the number of fires less than 0.2 ha in area.

Reconstruction of Earth images distorted by atmospheric scattering effects

In thematic mapping of aerospace images of the Earth's surface by use of the algorithms of automatic classification and image recognition, an important task is preliminary image processing for the purpose of removing distortions caused by aerosol component of the atmosphere (hazes, semitransparent fogs, and clouds). Usually, the image correction is difficult to make because the atmospheric transfer operator,

determined by atmospheric pulsed response or point spread function (PSF) is unknown. In many applications, it is necessary to estimate or reconstruct this function using information inherent in the observed image itself. Here, we tackle the problem of adaptive PSF retrieval from the information extracted from a blurred image. It is *a priori* assumed that in the observed fragment the physical object on the Earth's surface have distinct boundaries. Thus, the solution of this problem splits into the following steps[11,12]:

– a relatively stationary (in the sense that its PSF changes little in the shape) fragment of the image is selected;

– this image is differentiated, and the results are used to plot frequency distribution of gradients;

– taking into account the Gumbel's law of distribution of extreme values, the obtained histogram is split into two histograms. One describes the case with gradient, and the other without it;

– after the mixture is identified, the "ayes decision rule is constructed to test two hypotheses: the hypothesis H_1 of extreme gradients, and the hypothesis H_0 assuming no gradients present;

– the fragments of the video data belonging to the H_1 class are scanned, and the degree of their degradation is determined;

– the deconvolution is made using a standard procedure.

An example of applying this scheme is presented in Fig. 3.

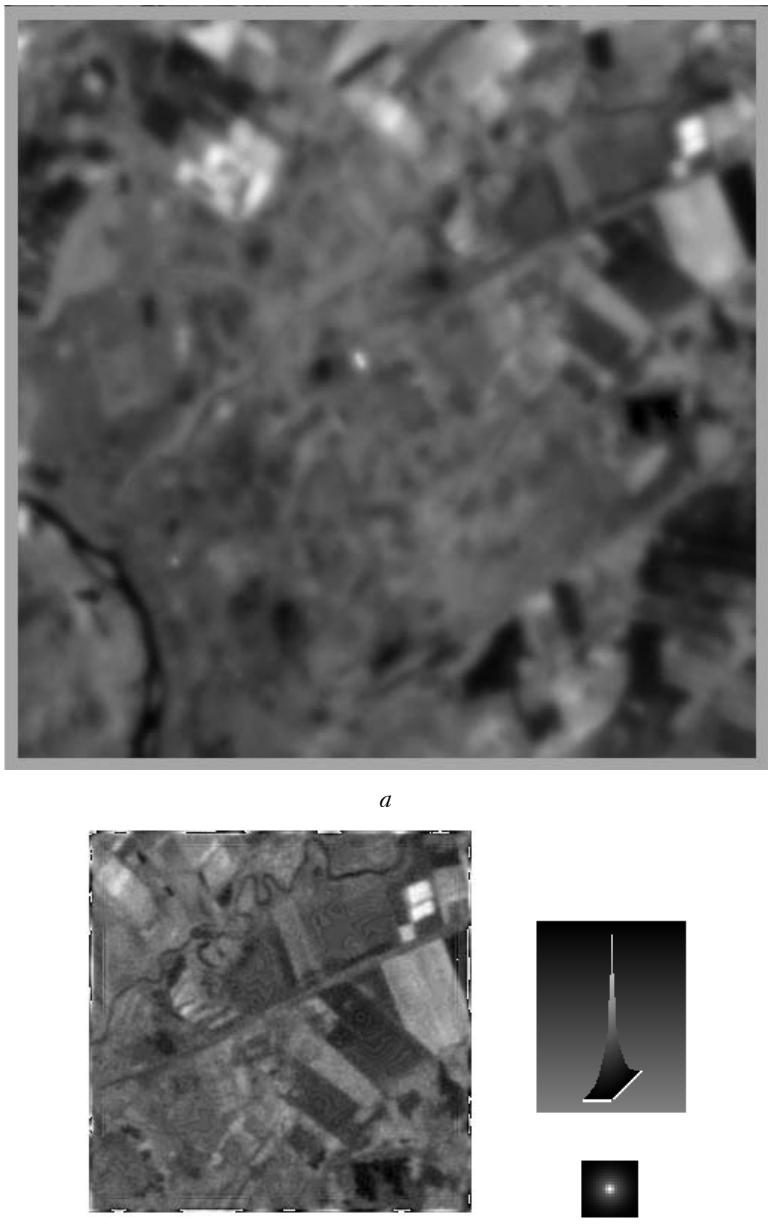

a

b

Fig. 3. Turbid image acquired by Resource satellite (top) and reconstructed fragment of an image (bottom).

0235-6880/99/10 951-06 $02.00

Problems with analysis of video data obtained for surface regions with fragmented semitransparent haze layers and/or cloudiness have been abundant. We propose two approaches to solving the problem of reconstructing images of the Earth's surface taken by AVHRR radiometer from onboard a NOAA satellite. The approach based on the histogram transformation works quite well when the observed image has undergone distorting effect of a semitransparent aerosol formation and when, in addition, a histogram of the brightness distribution is known for this or another, texturally similar segment of video data, obtained under conditions of high visibility. We will assume that, under ideal observation conditions, some section of the Earth surface will have brightness distribution described by the histogram $\hat{g}(y)$, and that a semitransparent fog distorts the $\hat{g}(y)$ histogram so that the resulting brightness distribution $\hat{f}(y)$ is observed. To reconstruct the image, the transformation $y = T(x)$ y, $x \in [0,1]$, is constructed that maps the brightness distribution $\hat{f}(y)$ of a distorted image onto the distribution $\hat{g}(y)$ mimicking the situation of "better" observation conditions and, thereby, reconstructs the turbid image. Another approach to video data reconstruction is based on regression analysis. To construct the regression equation, one has to have an image fragment with minimum distortion and with point-to-point correspondence to the image section to be reconstructed. "esides, to adapt the equation to specific conditions of observations, a section of undistorted image must be available in two channels simultaneously. To reconstruct the regression relationship in this case, the non-parametric statistical methods, usable to treat the nonlinear dependences, are employed.

Conclusion

The results of the studies dealing with the problem of thematic mapping and atmospheric correction of aerospace images are presented; they outline the main directions of the research carried out at the Institute of Atmospheric Optics S" RAS. This research was preceded and supplemented by analysis of influence the scattering and absorbing media produce on the image formation and transfer through such media. The results are summarized in Ref. 13.

Further study related to the problem of processing of multispectral aerospace images of the Earth's surface and atmosphere is planned to span the following directions:

1) atmospheric correction, i.e., creation of algorithmic facilities capable of filtering out the atmospheric distortions of the image to be subject to thematic mapping;

2) construction of algorithms of thematic mapping of the images, adapted to the case of significant atmospheric distortion and usable to solve such problems as early forest fire detection through semitransparent or broken clouds among others;

3) development of the methods for estimating the optical and physical state of the atmosphere and its composition from images of the Earth's surface taken from satellites in the optical wavelength range.

Acknowledgments

Authors would like to thank Academician V.E. Zuev, the consultant of the Presidium of RAS, the founder of the Institute of Atmospheric Optics S" RAS, for his stimulation and support of the research in this area and for providing the instrumentation (including ScanEx station) that has made this study possible.

References

1. B.S. Zhukov, Kosmicheskii Byulleten' **2**, No. 2, IV–VI (1995).
2. Y.J. Kaufman, Proc. SPIE **475**, *Remote Sensing*, 20–23 (1984).
3. V.V. Belov, S.V. Afonin, and I.Yu. Makushkina, Atmos. Oceanic Opt. **10**, Nos. 4–5, 278–288 (1997).
4. A. Werbowetzki, ed., *Atmospheric Sounding User's Guide*, NOAA Technical Report NESS 83 U.S. Department of Commerce National Oceanic and Atmospheric Administration, Washington, D.C. (1981), 83 pp.
5. C.R.N. Rao, L.L. Stowe, and E.P. McClain, Int. J. Remote Sensing **10**, Nos. 4–5, 743–749 (1989).
6. L.L. Stowe, Glob. and Planet. Change **4**, Nos. 1–3, 25–32 (1991).
7. V.V. Belov, S.V. Afonin, B.D. Belan, et al., in: *Proceedings of the Third Interrepublic Symposium on Atmospheric and Oceanic Optics* (Tomsk, 1996), pp 62–63.
8. Y.J Kaufman. C. Justice, *MODIS ATBD: Fire Products (Version 1.2.2 February 21 1994)*/EOS ID#2741. March 10, 1994, 47 pp.
9. N.A. Abushenko, N.P. Min'ko, S.M. Semenov, S.A. Tashchilin, and A.V. Tatarnikov, in: *Proceedings of the International School of Young Scientists and Specialists on Environmental Physics*, (Tomsk, June 14–23, 1999), pp. 46–49.
10. *ScanViewer* (Version 3.40), Description of the supplement to the preliminary image processing for receiving stations ISC ScanEx. Appendix A, p. A–13.
11. V.V. Belov, N.V. Molchunov, and K.T. Protasov, Atmos. Oceanic Opt. **10**, No. 7, 499–502 (1997).
12. G. Khan and S. Shapiro, *Statistical Models in Engineering Problems* (Mir, Moscow, 1969), 369 pp.
13. V.E. Zuev, V.V. Belov, and V.V. Veretennikov, *System Theory in Optics of Disperse Media* (SB RAS Press, Novosibirsk, 1997), 402 pp.